STOCHASTIC HOMOGENIZATION OF POLYMERIC FOAMS

Jörg Hohe
Fraunhofer Institut für Werkstoffmechanik, Wöhlerstr. 11, 79108 Freiburg, Germany
joerg.hohe@iwm.fraunhofer.de

Abstract The present study is concerned with a probabilistic homogenization analysis of polymeric cellular media to be used as core materials for sandwich structures. The approach is based on a randomized representative volume element in conjunction with a Monte Carlo simulation. The results for stiffness and strength are evaluated by stochastic methods.

Keywords: foam mechanics, disordered microstructures, homogenization, stochastic methods, large deformation.

1. INTRODUCTION

Solid polymeric foams are common core materials in modern sandwich construction. Their main advantages are their low specific weight due to their high void volume fraction, their low cost and the fact that foam core sandwich structures can be manufactured in a wide range of geometries.

For reasons of numerical efficiency, the analysis of cellular solids during the industrial design process is preferrably performed in terms of macroscopic effective properties rather than by a direct model of the given microstructure. The determination of the effective properties can be performed either by experiments or by numerical homogenization analyses. Since the pioneering work of Gent and Thomas [5] appeared in 1963, numerous studies on the theoretical determination of effective mechanical properties of foams have been published. Overviews are given e.g. by Gibson and Ashby [6] or Hohe and Becker [8] and others.

Although solid foams are amorphous media with a highly disordered microstructure (see e.g. experimental studies by Blazy et al. [1] and Ramamurty and Paul [11] showing distinct disorder effects), most of the analytical studies available in literature are based on idealized regular periodic foam models. Only few studies have been performed concerning irregular, random microstructures. Based on a Voronoi tessalation of a large scale representative

O.T. Thomsen et al. (eds), Sandwich Structures 7: Advancing with Sandwich Structures and Materials, 925–934.

volume element, e.g. Silva et al. [12] and van der Burg et al. [13] have analyzed the effect. More recent contributions have been published, among others, by Fazekas et al. [3] and Zhu et al. [15].

On the other hand, it has been pointed out by Fortes and Ashby [4] that a single analysis of a large-scale representative volume element with a random microstructure might be inaccurate since, artificial anisotropies are retained. Instead, a direct probabilistic approach based on a probability function for cell wall orientations is proposed. Other probabilistic approaches have been provided by Cuitiño and Zheng [2], Hall [7] as well as by Warren and Kraynik [14].

The present study is concerned with an alternative probabilistic approach where a previously developed homogenization procedure for periodic media under finite deformation [9] is generalized to cellular solids with a random microstructure. The basic idea of this approach is to determine the exact spatial positions of the cell wall intersections of a cellular solid randomly within prescribed areas. The analysis is performed in multiple numerical experiments which are evaluated by means of stochastic methods.

2. HOMOGENIZATION PROCEDURE FOR PERIODIC MODEL FOAMS

The probabilistic homogenization procedure presented in Section 3 generalizes a homogenization procedure for polymeric model foams with a periodic microstructure presented previously (Hohe and Becker [9]). The approach is based on the analysis of a representative volume element for the given microstructure according to Figure 1. For comparison, a virtual volume element of the same shape and size consisting of the homogenized "effective" medium is considered. The properties of the homogeneous volume element have to chosen such that the macroscopic mechanical behavior of both volume elements is equivalent.

The macroscopic mechanical equivalence of both volume elements is defined by the condition that the average strain energy densities $\bar{w}$ and $\bar{w}^*$ in both volume elements have to be equal

$$\bar{w} = \frac{1}{V^{\mathrm{RVE}}} \int\limits_{\Omega^{\mathrm{RVE}}} w \, \mathrm{d}V = \frac{1}{V^{\mathrm{RVE}}} \int\limits_{\Omega^{\mathrm{RVE}*}} w^* \, \mathrm{d}V = \bar{w}^* \tag{1}$$

provided that both volume elements experience a deformation which is equivalent on the macroscopic level of structural hierarchy. The deformation of both volume elements is defined to be macroscopically equivalent, if the volume averages

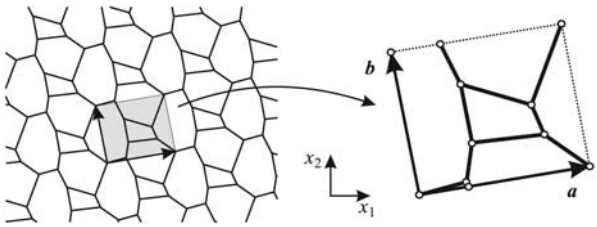

Figure 1. Deterministic two-dimensional cellular microstructure (periodic).

$$\bar{F}_{ij} = \frac{1}{V^{\mathrm{RVE}}} \int\limits_{\Omega^{\mathrm{RVE}}} F_{ij}\, \mathrm{d}V = \frac{1}{V^{\mathrm{RVE}}} \int\limits_{\Omega^{\mathrm{RVE}*}} F^*_{ij}\, \mathrm{d}V = \bar{F}^*_{ij} \tag{2}$$

of the components $F_{ij} = \partial u_i / \partial x_j + \delta_{ij}$ of the deformation gradient are equal.

The components of the deformation gradient are related to the components $\bar{\gamma}_{ij}$ of the macroscopic Green–Lagrange strain tensor by

$$\bar{\gamma}_{ij} = \frac{1}{2} \left(\bar{F}_{ki}\, \bar{F}_{kj} - \delta_{ij} \right) \tag{3}$$

where δ_{ij} are the components of the unit tensor. The components $\bar{\tau}_{ij}$ of the effective second Piola-Kirchhoff stress tensor can be determined from the average strain energy density as the partial derivatives

$$\bar{\tau}_{ij} = \frac{\partial \bar{w}}{\partial \bar{\gamma}_{ij}} \quad \approx \frac{\Delta \bar{w}}{\Delta \bar{\gamma}_{ij}} \tag{4}$$

if a hyperelastic material behavior is postulated.

A homogenization scheme based on Equations (1) to (4) basically requires the following four steps:

- identification of an appropriate representative volume element,
- deformation of a numerical (e.g. finite element) model of the representative volume element according to the prescribed effective strain state $\bar{\gamma}_{ij}$ considering Equation (3),
- computation of the strain energy density for the prescribed strain state and the corresponding partial derivatives,
- determination of the effective second Piola-Kirchhoff stress components $\bar{\tau}_{ij}$ using Equation (4).

Details on the implementation of this procedure can be found in the original contributions by Hohe and Becker [9, 10].

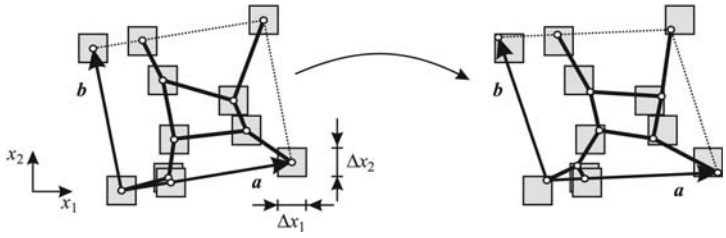

Figure 2. Randomized two-dimensional cellular microstructure.

3. PROBABILISTIC APPROACH

The concept for homogenization of perfectly periodic microstructures outlined in Section 2 is now enhanced to cover the effect of microstructural irregularity. For this purpose, the microstructure is randomized prior to the homogenization analysis. The randomization is performed by determining the exact spatial positions $x_i^{\mathrm{int}(j)}$ of cell wall intersections j, $(j = 1, \ldots, n)$ randomly within prescribed areas around the positions $x_i^{\mathrm{int,reg}(j)}$ of the corresponding perfectly regular microstructure using a random number generator (see Figure 2). In this context, the spatial dimensions Δx_i form additional material parameters discribing the degree of microstructural disorder. In most cases, the choice of equal spatial dimensions Δx_i of the cubes for random determination of the cell wall intersections will be appropriate. The single remaining parameter Δx can easily be determined from micrographic analyses of the respective solid foam.

The random determination of the microstructural geometry and the subsequent homogenization analysis are repeated in a number of numerical experiments. The results are evaluated by means of stochastic methods. Therefore, the effective stress $\bar{\tau}_{ij}$ for a given macroscopic strain state $\bar{\gamma}_{ij}$ is given in terms of the mean value

$$\bar{\tau}_{ij}^{\mathrm{a}} = \frac{1}{n} \sum_{k=1}^{n} \bar{\tau}_{ij}^{(k)} \tag{5}$$

where $\bar{\tau}_{ij}^{(k)}$ is the effective stress obtained in n individual numerical experiments. The scatter in the effective stress-strain relation can be assessed in terms of the standard deviation

$$\bar{\tau}_{ij}^{\mathrm{s}} = \left(\frac{1}{n-1} \sum_{k=1}^{n} \left(\bar{\tau}_{ij}^{\mathrm{a}} - \bar{\tau}_{ij}^{(k)} \right)^2 \right)^{\frac{1}{2}} \tag{6}$$

or the probability density distribution of the effective stresses.

For determination of the probability density distributions, the stress results $\bar{\tau}_{ij}^{(k)}$ from the individual numerical experiments are arranged in increasing or-

der. In this case, the accumulated probability $P(\bar{\sigma}_{ij})$ for the occurrence of a stress level of at least $\bar{\sigma}_{ij}$ is

$$P(\bar{\sigma}_{ij}) = \frac{k^* - \frac{1}{2}}{n} \tag{7}$$

where k^* is the number of the numerical experiment with $\bar{\sigma}_{ij}^{(k^*)} = \bar{\sigma}_{ij}$ after the re-arrangement of the stress results into increasing order whereas n is the total number of numerical experiments performed. From the accumulated probability $P(\bar{\sigma}_{ij})$, the probability density distribution is determined by

$$p(\bar{\sigma}_{ij}) = \frac{\partial P(\bar{\sigma}_{ij})}{\partial \bar{\sigma}_{ij}} \quad \left(= \frac{\Delta P(\bar{\sigma}_{ij})}{\Delta \bar{\sigma}_{ij}} \right) \tag{8}$$

where the partial derivative has to be computed numerically.

Advantage of the present probabilistic approach compared to the standard approaches based on the single analysis of a large-scale representative volume element is that not only the mean values of the effective stresses are obtained but additional information about the corresponding scatter bands is derived. The scatter can either be assessed in terms of the standard deviation or directly by determination of the probability density distribution. Therefore, the scheme provides an efficient and easy-to-use procedure for the numerical homogenization of random microstructures.

4. EXAMPLE: TWO-DIMENSIONAL MODEL FOAM

As an example, the effective behavior of a two-dimensional model foam is considered. As a periodic reference microstructure, a regular two-dimensional hexagonal honeycomb is employed. The cell wall material is described by an Ogden type constitutive equation

$$\begin{aligned} w &= \sum_{k=1}^{n} \frac{\mu_{(k)}}{\alpha_{(k)}} \left(\left(\lambda_1^{\mathrm{dev}}\right)^{\alpha_{(k)}} + \left(\lambda_2^{\mathrm{dev}}\right)^{\alpha_{(k)}} + \left(\lambda_3^{\mathrm{dev}}\right)^{\alpha_{(k)}} - 3 \right) \\ &\quad + \sum_{k=1}^{n} \kappa_{(k)} \, (J-1)^{2k} \end{aligned} \tag{9}$$

with

$$\lambda_k^{\mathrm{dev}} = J^{-\frac{1}{3}} \lambda_k$$

where λ_k and J are the principal values of the deformation gradient and the corresponding Jacobian respectively. The material parameters are assumed as $n = 2$ with $\alpha_1 = 1.5$, $\mu_1 = 1.4\,\mathrm{GPa}$ and $\kappa_1 = 0.8\,\mathrm{GPa}$ as well as $\alpha_2 = 3$, $\mu_2 = 1\,\mathrm{GPa}$ and $\kappa_2 = 0$ which might be assumed as being within the typical range for polymeric materials.

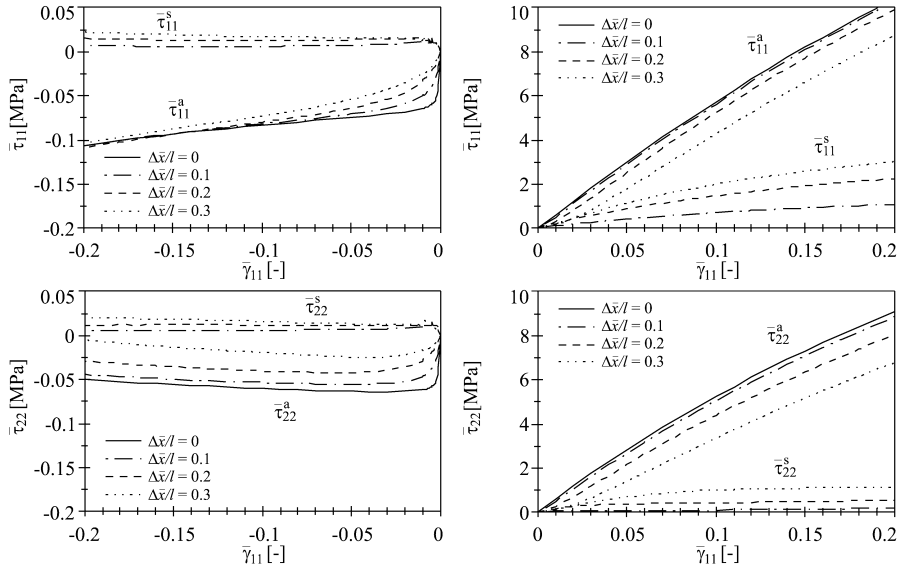

Figure 3. Macroscopic stress-strain relations for uniaxial compression and tension.

Although for simplicity all subsequent examples are related to two-dimensional microstructures, it should be noticed that the approach presented in Sections 2 and 3 can be applied to three-dimensional microstructures in the same manner.

5. EFEECTIVE STRESS-STRAIN RELATIONS

As a first example, the macroscopic stress-strain relations of the two-dimensional model foam characterized in Section 4 are analyzed. As an example, the load cases of a uniaxial tensile and compressive deformation are considered. In this context, the normal Green–Lagrange effective strain component $\bar{\gamma}_{11}$ is varied from zero level up to a level of 20% tensile or compressive strain respectively. The remaining in-plane components $\bar{\gamma}_{22}$ and $\bar{\gamma}_{12}$ of the macroscopic Green–Lagrange strain tensor are assumed to vanish throughout the deformation history.

In Figure 3, the results are presented considering the effective normal stress component $\bar{\tau}_{11}$ acting within the direction of the applied macroscopic deformation as well as the net stress component $\bar{\tau}_{22}$ perpendicular to this direction. Three different levels $\Delta x/l$ of microstructural disorder are analyzed, where l is the (uniform) strut length for the reference model foam with regular hexagonal microstructure. Results for this case are indicated by a solid line in the respective plot.

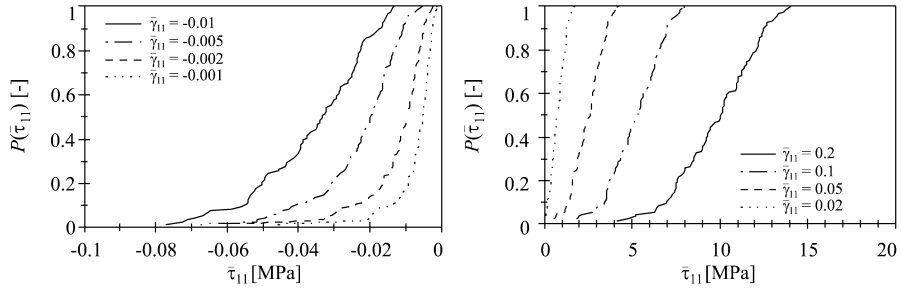

Figure 4. Distribution of the accumulated stress probability for different effective load levels.

It is observed that in the tensile range both, the nominal effective stress $\bar{\tau}_{11}$ as well as the net stress $\bar{\tau}_{22}$ decrease with increasing microstructural disorder. Thus, the increasing microstructural disorder leads to a weaker material response on the effective level of structural hierarchy, whereas the perfectly regular hexagonal foam model overestimates the effective stresses and thus the effectve stiffness of the material. This effect is caused by a transition in the microscopic mode of deformation. For the perfectly regular microstructure, the deformation under a uniaxial effective strain state is governed by cell wall stretching in the longitudinal direction of the individual struts. For increasingly disordered microstructures, localized bending of the struts in the vicinity of the cell wall intersections becomes more important, leading to a weaker macroscopic material response.

In the compressive range, strong effects of the microstructural disorder are observed especially at low levels $-\bar{\gamma}_{11}$ of the applied effective strain. In this range, the perfectly regular microstructure exhibits a branching instability in the effective material response caused by buckling of the cell walls. No such instability in the rigorous Eulerian sense occurs for disordered microstructures, resulting in a distinct weakening of the effective material in this range for increasing microstructural disorder.

The accumulated probability $P(\bar{\tau}_{11})$ for the occurence of an effective stress level of at least $\bar{\tau}_{11}$ is presented in Figure 4 at four different compressive and tensile deformation levels $\bar{\gamma}_{11}$. A constant degree $\Delta x/l = 0.2$ of the microstructural disorder is considered. In the tensile range, an increasing level of the applied effective deformation leads to a monotonic increase of both, the average effective stress $\bar{\tau}_{11}^{\mathrm{a}}$ and the scatter band width characterized by a decreasing slope of the accumulated probability P. In the compressive range, an additional transition of the curve shape of the accumulated stress probability is observed. At low effective stress levels, a bimodal behavior develops, where the range of a low gradient belongs to microstructures in the pre-buckled state whereas a the zone of a larger gradient of the accumulated probability at

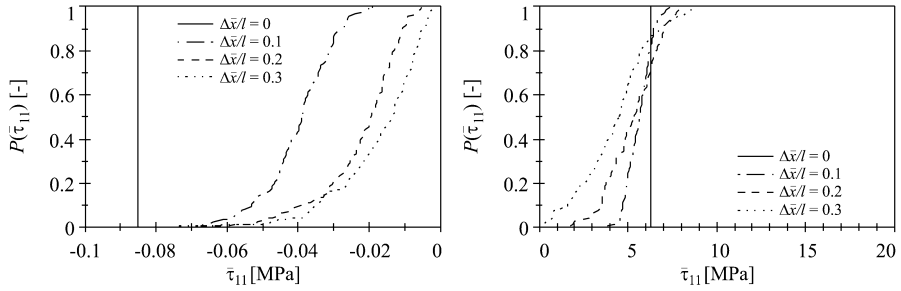

Figure 5. Distribution of the accumulated stress probability for different disorder degrees.

lower effective stress levels indicates a microstructural deformation mode in the postbuckling range.

The effect of the degree $\Delta x/l$ of microstructural disorder on the stress probability at fixed levels $\bar{\gamma}_{11} = -0.005$ and $\bar{\gamma}_{11} = 0.1$ is analyzed in Figure 5. Again, it is observed that an increasing degree of microstructural disorder does not only cause an increasing scatter of the results but also has distinct effects on the average stresses, resulting in a general weakening of the corresponding effective material.

6. EFEECTIVE STRENGTH

In a final investigation, the effective strength of ordered and disordered cellular solids is analyzed. In accordance with the weakest link concept, failure of the entire microstructure is assumed if the first strut in the representative volume element fails. Failure of the struts is assessed by a simple maximum stress criterion assuming a maximum permitted v. Mises stress of $\sigma_e = 125\,\text{MPa}$. From the effective stress-strain curves, the failure strain $\bar{\gamma}_{ij}^{f}$ on the effective level is computed as the effective strain, where the local failure criterion is first satisfied anywhere in the representative volume element.

The results for uniaxial compressive and tensile deformation within the x_1- and x_2-directions are presented in Figure 6. It is observed that an increasing degree $\Delta x/l$ of microstructural disorder leads to a distinct decrease of the effective failure load in the tensile range by about 30%. In the compressive range, the consideration of the microstructural disorder results in the vanishing of the strength anisotropy of the perfectly regular microstructure with different effective failure stresses $\bar{\gamma}_{11}^{f}$ and $\bar{\gamma}_{22}^{f}$ within the x_1- and x_2-directions.

7. CONCLUSION

The present study provides a simple analytical scheme for the homogenization analysis of solid foams accounting especially for the microstructural disorder. The scheme is based on a Monte Carlo simulation of randomized

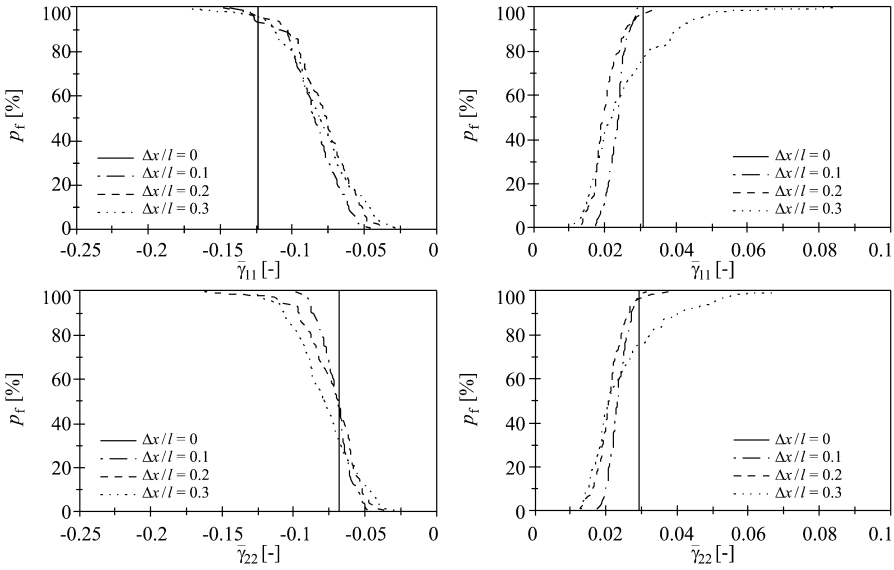

Figure 6. Accumulated failure probability under tensile and compressive deformation.

small-scale representative volume elements in conjunction with a strain energy based approach for the homogenization analysis.

Advantage of the approach is that it fully accounts for the misrostructural irregularity. Due to its formulation in terms of numerical experiments in conjunction with a stochastic assessment, both, the average properties of the effective material as well as the scatter can be assessed, which is impossible in the previeous approaches based on a single analysis of a large-scale representative volume element consisting of a huge number of base cells.

In a number of numerical examples considering both the effective stress-strain response of random cellular solids as well as their effective strength, it is observed that the microstructural disorder does not only affect the scatter to be expected in the respective effective material properties but also can have distinct effects on the respective average values. In general, an increasing degree of microstructural disorder results in a general weakening of the effective material behavior in terms of both, the effective stiffness and the effective strength. Both of these quantities are overestimated by a classical approach based on a perfectly regular, periodic model for the cellular microstructure.

REFERENCES

[1] J.S. Blazy, A. Marie-Louise, S. Forest, Y. Chastel, A. Pineau, A. Awade, C. Grolleron and F. Moussy, F. Deformation and fracture of aluminium foams under proportional and multi-axial loading: statistical analysis and size effect. *International Journal of the Mechanical Sciences* 46:217-244, 2004.

[2] A.M. Cuitino and S. Zheng. Taylor averaging on heterogeneous foams. *Journal of Composite Materials* 37:701-713, 2003.

[3] A. Fazekas, R. Dendievel, L. Salvo and Y. Bréchet. Effect of microstructural topology upon the stiffness and strength of 2D cellular structures. *International Journal of the Mechanical Sciences* 44:2047-2066, 2002.

[4] M.A. Fortes and M.F. Ashby. The effect of non-uniformity on the in-plane modulus of honeycombs. *Acta Materialia* 47:3469-3473, 1999.

[5] A.N. Gent and A.G. Thomas. Mechanics of foamed elastic materials. *Rubber Chemistry and Technology* 36:597-610, 1963.

[6] L.J. Gibson, and M.F. Ashby. *Cellular Solids – Structure and Properties*. Cambridge University Press, London 1997.

[7] R. Hall. Effective moduli of cellular materials. *Journal of Reinforced Plastics and Composites* 12:186-197, 1993.

[8] J. Hohe and W. Becker. Effective stress-strain relations for two-dimensional cellular sandwich cores: Homogenization, material models and properties. *Applied Mechanics Reviews* 55:61-87, 2002.

[9] J. Hohe and W. Becker. Effective mechanical behavior of hyperelastic honeycombs and two-dimensional model foams at finite strain. *International Journal of the Mechanical Sciences* 45:891-913, 2003.

[10] J. Hohe and W. Becker. A probabilistic approach to the numerical homogenization of irregular solid foams at finite strain. *International Journal of Solids and Structures* 42:3549-3569, 2005.

[11] U. Ramamurty and A. Paul. Variability in mechanical properties of a metal foam. *Acta Materialia* 52:869-876, 2004.

[12] M.J. Silva, W.C. Hayes and L.J. Gibson. The effects of non-periodic microstructure on the elastic properties of two-dimensional cellular solids. *International Journal of the Mechanical Sciences* 37:1161-1177, 1995.

[13] M.W.D. van der Burg, V. Shulmeister, E. van der Giessen and R. Marissen. On the linear elastic properties of regular and random open-cell foam models. *Journal of Cellular Plastics* 33:31-54, 1997.

[14] W.E. Warren and A.M. Kraynik. Linear elastic behavior of a low-density Kelvin foam with open cells. *Journal of Applied Mechanics* 64:787-794, 1997.

[15] H.X. Zhu, J.R. Hobdell and A.H. Windle. Effects of cell irregularity on the elastic properties of 2D Voronoi honeycombs. *Journal of the Mechanics and Physics of Solids* 49:857-870, 2001.